

## Supporting Information

### Selective electroreduction of CO<sub>2</sub> to formate by a heterogenized Ir complex using H<sub>2</sub>O as an electron/proton source

Jieun Jung,<sup>\*a</sup> Keun Woo Lee,<sup>‡a</sup> Naonari Sakamoto,<sup>‡b</sup> Selvam Kaliyamoorthy,<sup>‡a</sup> Taku Wakabayashi,<sup>a</sup> Kenji Kamada,<sup>a</sup> Keita Sekizawa,<sup>b</sup> Shunsuke Sato,<sup>b</sup> Tomiko M. Suzuki,<sup>b</sup> Takeshi Morikawa<sup>b</sup> and Susumu Saito<sup>\*ac</sup>

<sup>a</sup> *Department of Chemistry, Graduate School of Science, Nagoya University, Chikusa, Nagoya 464-8602, Japan*

<sup>b</sup> *Toyota Central R&D Labs., Inc., 41-1 Yokomichi, Nagakute, Aichi 480-1192, Japan*

<sup>c</sup> *Integrated Research Consortium on Chemical Science (IRCCS), Nagoya University, Chikusa, Nagoya 464-8602, Japan*

<sup>‡</sup> *These authors contributed equally to this work.*

<sup>\*</sup>To whom correspondence should be addressed.

E-mail: jung.jieun.z7@f.mail.nagoya-u.ac.jp, saito.susumu.c4@f.mail.nagoya-u.ac.jp

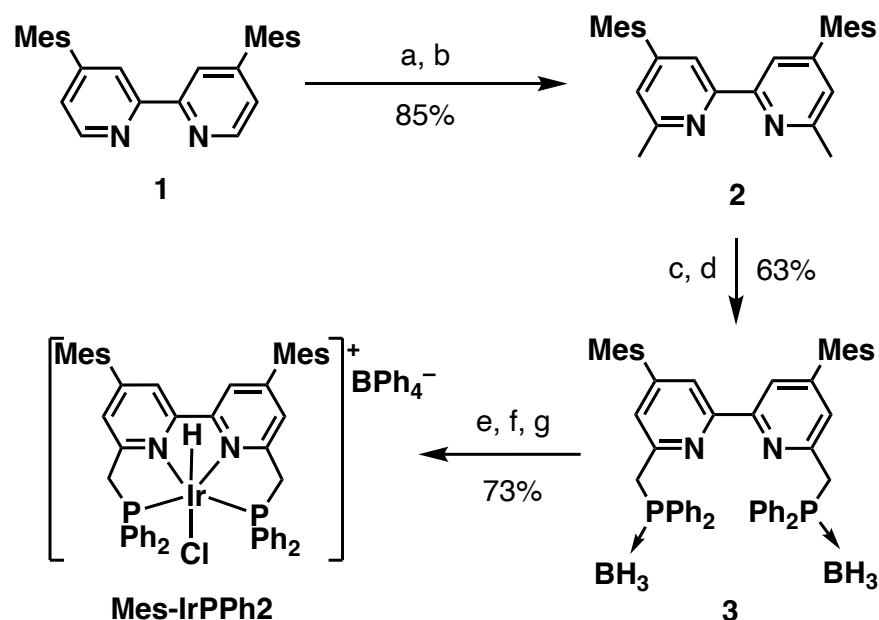
## Experimental section

**Generals.** All experiments were performed under an Ar atmosphere unless otherwise noted.  $^1\text{H}$  NMR spectra were recorded on a JEOL ECA-600 (600 MHz for  $^1\text{H}$ ) and JEOL ECA-500 (500 MHz for  $^1\text{H}$ ) at ambient temperature. Chemical shifts are reported as  $\delta$  in ppm and are internally referenced to tetramethylsilane (0.0 ppm for  $^1\text{H}$ ). The following abbreviations are used: s = singlet, d = doublet, t = triplet, q = quartet, br = broad, dd = doublet of doublet, and m = multiplet.  $^{31}\text{P}$  NMR spectra were measured on JEOL ECA-600 (243 MHz) at ambient temperature unless otherwise noted. Chemical shifts are reported in ppm from the solvent resonance employed as the external standard (phosphoric acid (85 wt% in  $\text{H}_2\text{O}$ ) at 0.0 ppm). High-resolution mass spectra (HRMS) were recorded on PE Biosystems QSTAR (electrospray ionization mass spectroscopy (ESI-MS)). For thin-layer chromatography (TLC) analysis through this work, Merck pre-coated TLC plates (silica gel 60 GF254 0.25 mm) were used. The products were purified by preparative column chromatography on silica gel 60 N (spherical, neutral) (40–100  $\mu\text{m}$ ; Kanto).

**Materials.** Commercially available chemicals were used without further purification unless otherwise indicated. Methyllithium (3 M in diethoxymethane), diisopropylamine, 1,10-phenanthroline, ammonium tetrphenylborate, and Carbon- $^{13}\text{C}$  dioxide were purchased from Aldrich Chemical Co. Morpholine, *n*-BuLi (1.6 M in hexane), acetonitrile (MeCN, anhydrous), tetrahydrofuran (THF, anhydrous), methanol (anhydrous), diethyl ether (anhydrous), ethyl acetate, chloroform, deuterium oxide and celite were purchased from Kanto Chemicals, Ltd. Borane-tetrahydrofuran complex, ethanol (anhydrous), chlorodiphenylphosphine, chloroform-*d*, and hexane were purchased from FUJIFILM Wako Pure Chemical Corporation. Tetrabutylammonium hexafluorophosphate ( $\text{Bu}_4\text{NPF}_6$ ) was purchased from Tokyo Chemical Industry CO., Ltd. Chloro(1,5-cyclooctadiene)iridium(I) dimer was purchased from FURUYA METAL CO., LTD. Manganese(IV) dioxide was purchased from Merck. Carbon dioxide gas was purchased from Alpha system Co., Ltd.  $\text{D}_2\text{O}$  was purchased from Cambridge Isotope Laboratories, Inc. Ir complexes (Scheme S1, **IrPCY2**, **Mes-IrPCY2**, and **IrPPh2**) were synthesized according to the literatures.<sup>S1-S2</sup>

**Instrumentation.** Products obtained in the electrocatalytic reduction of CO<sub>2</sub> were analyzed by Micro-GC (Agilent 490) equipped with a thermal conductivity detector (column: MS5A 10-m BF column; isothermal at 80 °C; carrier gas: Ar), and Prominence Organic Acid Analysis System (SCR-102H Column; Column Temp.: 40 °C; Cell Temp.: 43 °C) or IC instrument (Dionex ICS-2000) with IonPacAS15 and Ion-PacAG15 columns. The column temperature was maintained at 308 K. A solution of 3 mM KOH was used as the first eluent up to 10 min, and then the eluent was changed gradually to 10 mM KOH over 5 min, followed by a change to 30 mM KOH solution over 5 min. Cyclic voltammetry (CV) measurements were carried out in a MeCN solution containing 0.10 M Bu<sub>4</sub>NPF<sub>6</sub> as an electrolyte at 298 K under Ar with use of a glassy carbon as a working electrode (3 mm diameter), a platinum wire as a counter electrode, and a Ag/AgNO<sub>3</sub> electrode (in a MeCN solution containing 0.10 M tetrabutylammonium perchlorate and 0.01 M AgNO<sub>3</sub>). The potentials were calibrated by the standard potential of ferrocene/ferrocenium (Fc/Fc<sup>+</sup>). Scanning electron microscope (SEM) images were taken with JEOL JSM-6610A microscopy with experimental parameters of SEI, AV = 20 kV, WD = 10 mm, SS = 62. Characterization Surface analysis using XPS (Ulvac Phi, Quantera SXM) was performed with a monochromatic Al K $\alpha$  X-ray source (1486.6 eV), a photoelectron take-off angle of 45°, an analysis area with a diameter of 200  $\mu$ m, and charge-up correction using the C 1s 285 eV peak. The structure of the complexes was determined using a time-of-flight mass spectroscopy system (TOFMS, JEOL JMS-T100LP) with a MeCN mixture as the mobile phase. For the analysis of the [Mes-IrPPh<sub>2</sub>] electrode following the CO<sub>2</sub>ERR, a 0.5  $\times$  0.5 cm<sup>2</sup> section was excised, extracted with CH<sub>3</sub>Cl, evaporated to remove the CH<sub>3</sub>Cl, redissolved in CH<sub>3</sub>CN, and diluted to the optimal concentration for ESI-MS.

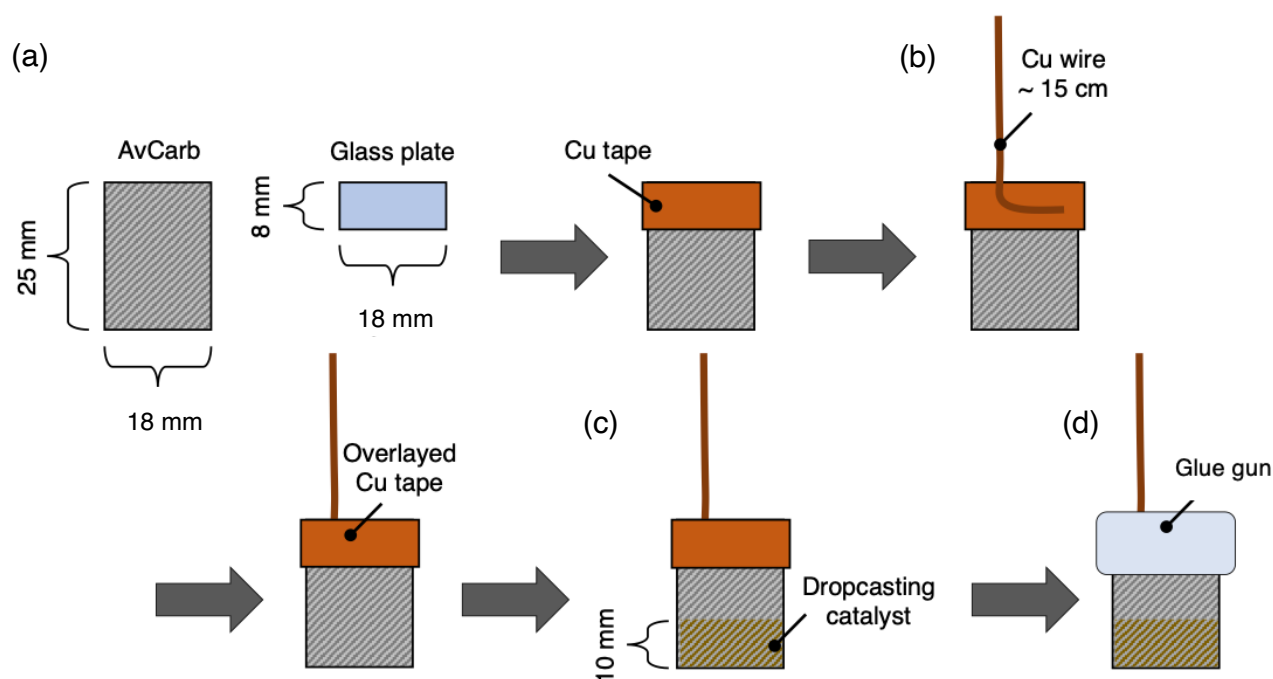
**Synthesis of chlorohydro(6,6'-bis((diphenylphosphino)methyl)-4,4'-bis(2,4,6-trimethylphenyl)-2,2'-bipyridine-iridium tetraphenyl borate (Mes-IrPPh<sub>2</sub>).** In a Schenk flask, 163.3 mg of 6,6'-bis((diphenylphosphino)methyl)-4,4'-bis(2,4,6-trimethylphenyl)-2,2'-bipyridine-diborane complex (0.2 mmol) was charged under Ar atmosphere equipped with a stirrer bar. 5 mL of degassed morpholine was added and refluxed at 120 °C for 2 h. Then, morpholine was removed *in vacuo* (ca. 0.1 mmHg, 70 °C). To the resulting residue, 67.2 mg (0.1 mmol) of chloro(1,5-cyclooctadiene)iridium(I) dimer and 7.2 mL of degassed methanol were added to the vessel and stirred at room temperature for overnight. The mixture was then refluxed at 70 °C for 3 h then cooled to room temperature. Celite filtration was conducted under an Ar atmosphere and the filtrate was collected in a separate Schlenk flask. 101.2 mg (0.3 mmol) of ammonium tetraphenylborate was added to the vessel and stirred at 50 °C for 5 h. The resulting yellow precipitation was filtered and washed with MeOH to afford **Mes-IrPPh<sub>2</sub>** as a slightly greenish yellow solid (0.1934 g, 73% yield). <sup>1</sup>H NMR (600 MHz, CDCl<sub>3</sub>): δ 7.66 (s, 2H), 7.50 (t, 2H, *J* = 7.3 Hz), 7.42 (t, 2H, *J* = 7.3 Hz), 7.37 (m, 4H), 7.30 (m, 8H), 7.21–7.24 (m, 6H), 7.06 (m, 4H), 6.97 (d, 4H, *J* = 17 Hz), 6.80 (t, 8H, *J* = 7.0 Hz), 6.72 (t, 4H, *J* = 6.9 Hz), 4.40 (m, 4H), 2.34 (s, 6H), 2.07 (s, 6H), 1.97 (s, 6H), -19.2 (t, 1H, *J* = 18 Hz). HRMS (ESI, (M-BPh<sub>4</sub>)<sup>+</sup>) Calcd for C<sub>54</sub>H<sub>51</sub>ClIrN<sub>2</sub>P<sub>2</sub><sup>+</sup>: 1017.2845. Found *m/z* = 1017.2868.



**Scheme S1** The synthesis of **Mes-IrPPh<sub>2</sub>**. Reagents: a) MeLi, THF; b) MnO<sub>2</sub>, CH<sub>2</sub>Cl<sub>2</sub>; c) LDA, PPh<sub>2</sub>Cl, THF; d) BH<sub>3</sub>-THF; e) morpholine; f) [Ir(cod)Cl]<sub>2</sub>, MeOH; g) NH<sub>4</sub>BPh<sub>4</sub>, MeOH.

**Preparation of (PNNP)Ir catalyst ink.** The synthesized Ir complexes were polymerized using a chemical method. Each Ir complex (13.4  $\mu\text{mol}$ ) and carbon black (Vulcan XC-72R, 15 mg) in a MeCN (2.9 mL) solution were mixed with chemical polymerization initiators, pyrrole solution (0.3 mL, 0.722 mM in a MeCN) and  $\text{FeCl}_3$  solution (0.562 mL, 200 mM in ethanol). The mixture was dispersed by ultrasonicator for 3 min for polymerization. The ink was evaporated completely *in vacuo* to obtain a black powder, which was then dispersed in a mixed solution of 2-propanol (1.112 mL) and Nafion (5 wt%, 0.106 mL) using a ultrasonicator to obtain a catalyst ink.

**Fabrication of [Ir-ink] cathode.** The catalyst was immobilized on a carbon material electrode using a chemical deposition and drop-cast method as depicted in Scheme S2. (a) A glass plate (8 mm  $\times$  18 mm) was attached to a carbon material electrode (25 mm  $\times$  18 mm) with a copper (Cu) tape. (b) A Cu wire was connected to the carbon material electrode using an additional Cu tape. (c) The catalyst ink (65  $\mu\text{L}$  at a time, 0.715  $\mu\text{mol}$  of [Ir]) was uniformly dropped onto 1.8  $\text{cm}^2$  of the carbon material electrode, and then dried at 70  $^\circ\text{C}$  for 3 min in a drying oven. This coating procedure was repeated several times (2–8 times) and the resulting electrode was rinsed with pure water and dried at room temperature until the moisture was completely evaporated. (d) Finally, glue gun was applied to mask the Cu tape surface to avoid interference during electroreduction of  $\text{CO}_2$ .



**Scheme S2** Schematic illustration of a working electrode preparation.

**Electrocatalytic CO<sub>2</sub> reduction.** Electrocatalytic CO<sub>2</sub> reduction reactions were performed at atmospheric pressure with a potentiostat. A two-compartment Pyrex cell separated with a proton exchange membrane (Nafion 117) was used as the reactor to prevent re-oxidation of the formate. The [Ir-ink] electrode was used as a working electrode where Ag/AgCl and coiled platinum wire were used as the reference and counter electrodes, respectively. The [Ir-ink] electrode was prepared with 2 times of drop-casting as the cathode unless otherwise noted. A rubber septum was deployed for the cathodic compartment to tightly prevent oxygen contamination as it was realized that the contamination causes deterioration of catalytic activity. 0.5 M KHCO<sub>3</sub> solution (140 mL) was used as the electrolyte unless otherwise noted. Then, CO<sub>2</sub> gas was bubbled into the reactor for 30 min prior to the measurement. To eliminate the capacitive current arising from between the working and counter electrodes, pre-electrolysis was conducted  $-0.07$  V *vs.* RHE (reversible hydrogen electrode) for 10 min prior to the electrocatalytic CO<sub>2</sub> reduction. The amounts of CO and H<sub>2</sub> in the gas phase were analyzed using a micro-GC (Agilent 490) equipped with a thermal conductivity detector (column: MS5A 10-m BF column; isothermal at 80 °C; carrier gas: Ar) while the liquid product (formate) was collected from the electrolyte solution and analyzed by Prominence Organic Acid Analysis System (SCR-102H Column; Column Temp.: 40 °C; Cell Temp.: 43 °C). The column temperature was maintained at 308 K. A solution of 3.0 mM KOH was used as the first eluent up to 10 min, and then the eluent was changed gradually to 10 mM KOH over 5 min, followed by a change to 30 mM KOH solution over 5 min.

**Calculation of potential values *vs.* RHE.** Potential values expressed *vs.* RHE were obtained using the following equation:

$$E \text{ vs. RHE} = E_a + 0.059 \text{ pH} + 0.195 \text{ (for Ag/AgCl in 3.0 M NaCl)} \quad (1)$$

$$E \text{ vs. RHE} = E_a + 0.059 \text{ pH} \text{ (for SHE; standard hydrogen electrode)} \quad (2)$$

$$E \text{ vs. RHE} = E_a + 0.059 \text{ pH} + 0.244 \text{ (for SCE; saturated calomel electrode)} \quad (3)$$

where  $E_a$  was applied potential.

The pH of the 0.5 M KHCO<sub>3</sub> solution saturated with CO<sub>2</sub> was approximately 7.3.

**Preparation of Ni/Fe-Ni foam.** An Ni/Fe-Ni foam anode electrode used for solar-driven CO<sub>2</sub> reduction was prepared by previously reported method with a minor modification.<sup>S3</sup> First, Ni foam was sonicated in 3.0 M HCl, acetone, and ethanol for 20 min, respectively. After drying in vacuum, Ni foam was dipped into an ethanol solution, which was prepared by dissolving 150 mg of NiCl<sub>2</sub>·6H<sub>2</sub>O and 75 mg of FeCl<sub>2</sub>·4H<sub>2</sub>O into 10 mL of ethanol. After dipping, catalyst coated Ni foam was dried in air at room temperature overnight. Then, Ni foam was calcined at 423 K for 2 h in air. After pre-electrolysis was carried out in 1.0 M KOH at 0.6 V vs. Ag/AgCl for 1 h, Ni/Fe-Ni foam anode for solar-driven CO<sub>2</sub> reduction was obtained.

**Solar-driven CO<sub>2</sub> reduction.** Solar-driven CO<sub>2</sub> reduction system was constructed comprising a [Mes-IrPPh<sub>2</sub>] cathode (10 cm<sup>2</sup>), an Ni/Fe-Ni foam anode (10 cm<sup>2</sup>) and four series-Si solar cell (1.6 cm<sup>2</sup>) (photovoltaic efficiency was 22.7%). Solar-driven CO<sub>2</sub> reduction trials were performed under a flow of 100% CO<sub>2</sub> in a two-compartment reactor separated by a Nafion117 cation membrane. A CO<sub>2</sub>-saturated aqueous solution containing 0.5 M KHCO<sub>3</sub> was used as the electrolyte at 308 K. The Si solar cell was exposed to simulated solar light from a HAL-320 device (Asahi Spectra Co., Ltd.) at an intensity of on sun. A following equation was used to calculate the solar-to-formate conversion efficiency values ( $\eta_{\text{STF}}$ ).

$$\eta_{\text{STF}} = (R_{\text{F}} \times \Delta G) / (I \times A) \times 100$$

R<sub>F</sub>: Mean rate of formate produced (7035.2 μmol/24 h)

ΔG: Change in Gibbs free energy per mole of formic acid produced from CO<sub>2</sub> and water (ΔG = 270 kJ/mol at 298 K)

I: Light intensity (100 mW cm<sup>-2</sup>)

A: Irradiation area (1.6 cm<sup>2</sup>)

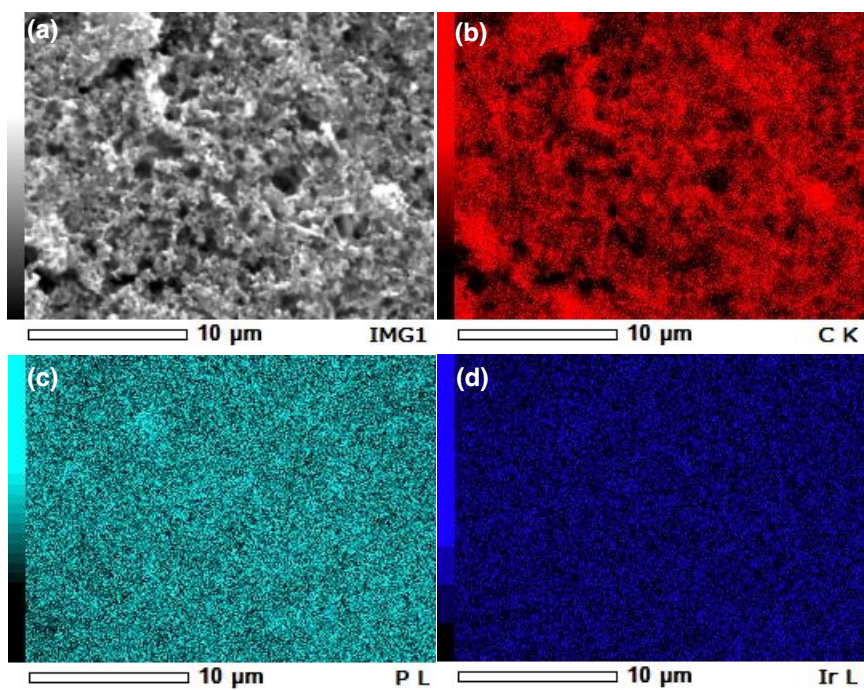


**Fig. S1** (a) A SEM image and elemental mapping [(b) C, (c) P, and (d) Ir elements] of a [**Mes-IrPPh<sub>2</sub>**] electrode; top view.

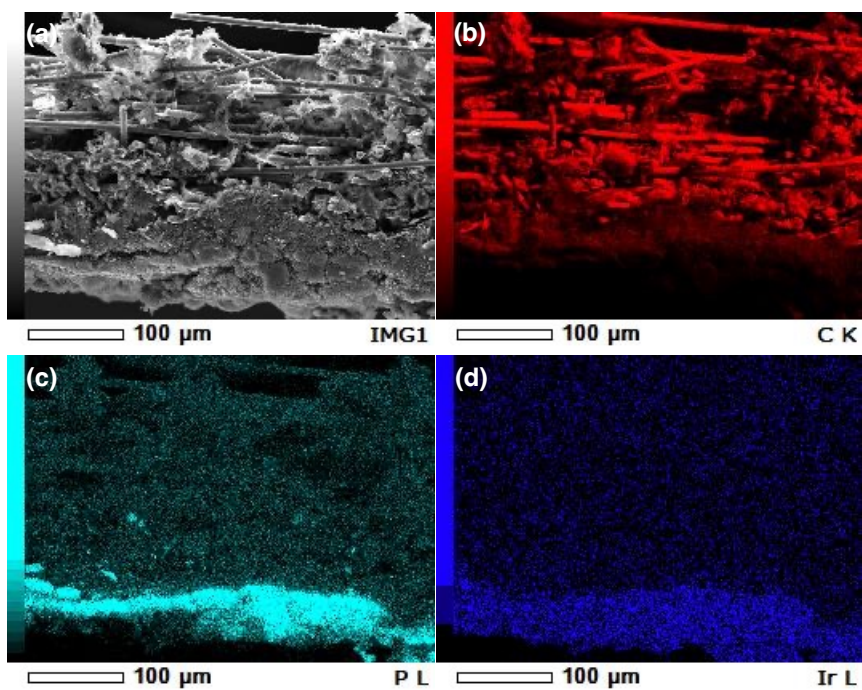


**Fig. S2** (a) A SEM image and elemental mapping [(b) C, (c) P, and (d) Ir elements] of a [**Mes-IrPPh<sub>2</sub>**] electrode; cross-section.

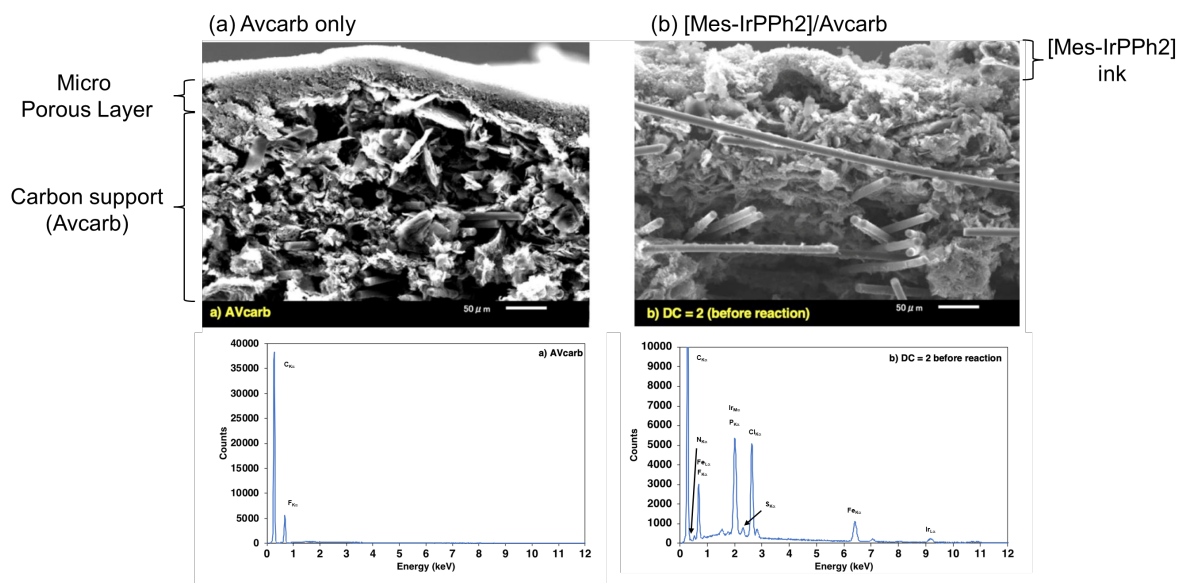


**Fig. S3** EDS (energy dispersive X-ray spectroscopy) cross-section analysis of (a) a bare Avcarb and (b) a [Mes-IrPPh2] electrode (Mes-IrPPh2/Avcarb).

Bare Avcarb (Avcarb GDS 3250) has a microporous layer and is water-repellent, which explains the presence of F, in addition to C. In the electrode coated with [Mes-IrPPh2] ink, the presence of Ir, Fe, P, Cl, and S was newly confirmed. The detection of Ir and P indicates the presence of Mes-IrPPh2 + polypyrrole, while S is attributed to the presence of Nafion (polytetrafluoroethylene + sulfonic acid). Fe and Cl are attributed to the residual FeCl<sub>3</sub> used in the polypyrrole polymerization process and the Cl ligand coordinated to Mes-IrPPh2.

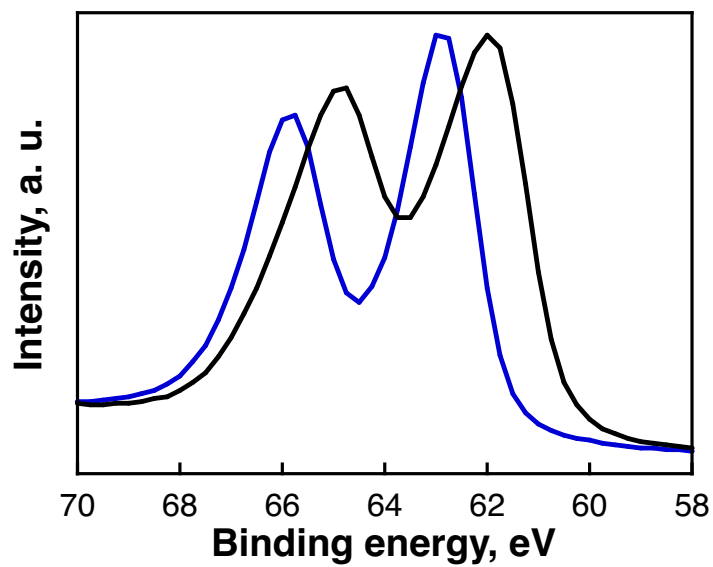
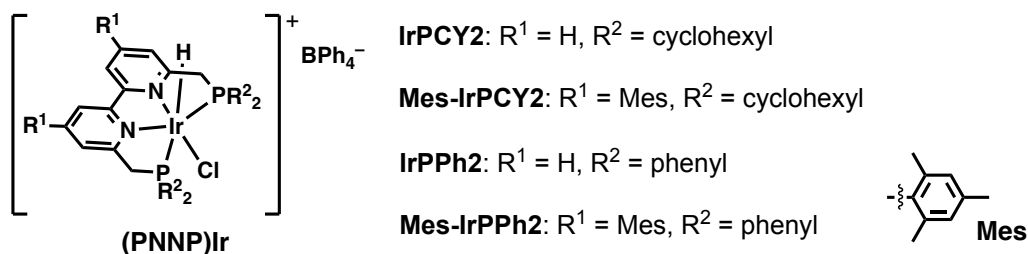


**Fig. S4** Ir 4f XPS spectra of Ir(III)Cl<sub>3</sub>•H<sub>2</sub>O (blue; located at 63 and 66 eV) and [Ir(I)(1,5-cod)Cl]<sub>2</sub> (black; located at 62 and 65 eV).

**Table S1** Electrocatalytic CO<sub>2</sub> reduction with a PNNP-type Ir complex immobilized on a carbon material ([Ir-ink] electrode)



Entry	Complex	Product, $\mu\text{mol}$ (FE, %)			$j$ , $\text{mA cm}^{-2}$
		HCOO <sup>-</sup>	CO	H <sub>2</sub>	
1	<b>IrPCY2</b>	31 (49)	1.8 (2.7)	41 (64)	0.63
2	<b>IrPPh2</b>	18 (45)	4.2 (11)	6.9 (17)	0.40
3	<b>Mes-IrPCY2</b>	244 (88)	13 (16)	21 (7.6)	2.74
4	<b>Mes-IrPPh2</b>	732 (86)	32 (3.8)	10 (1.2)	5.49

Pre-electrolysis at  $-0.07$  V vs. RHE for 10 min; electrolysis at  $-0.37$  V vs. RHE for 3 h in a 0.5 M KHCO<sub>3</sub> solution (Drop-casting counts: 2 times for each)

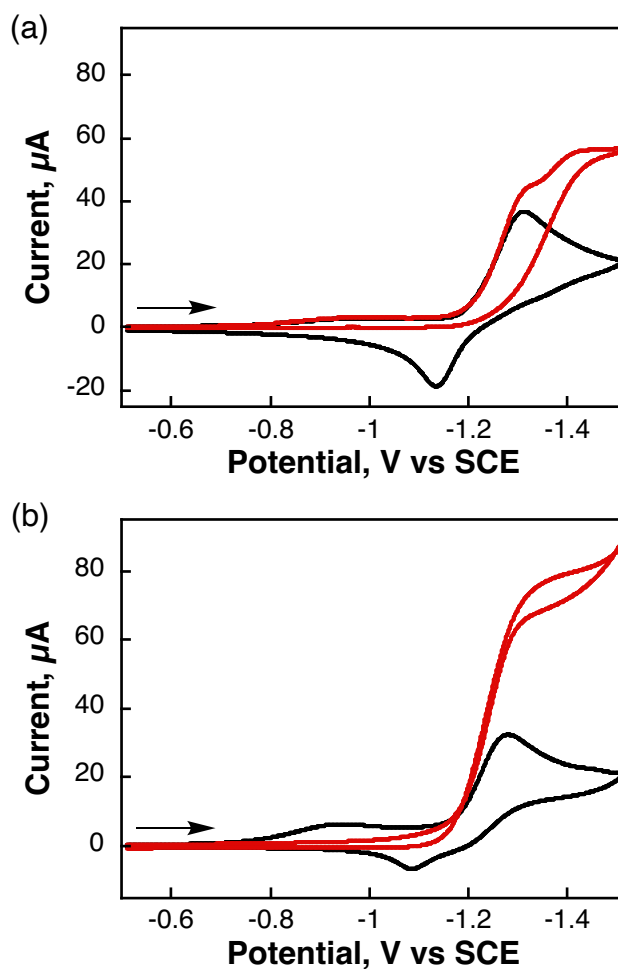


**Fig. S5** Cyclic voltammograms of (a) **Mes-IrPCY2** (1.0 mM) and (b) **Mes-IrPPh2** (1.0 mM) in a MeCN solution containing  $\text{Bu}_4\text{NPF}_6$  (0.10 M) as a supporting electrolyte under Ar (black) and (b)  $\text{CO}_2$  (red) atmospheres at 298 K. Scan rate =  $0.1 \text{ V s}^{-1}$ .

**Table S2** Electrocatalytic CO<sub>2</sub> reduction with a [Mes-IrPPh<sub>2</sub>] electrode using different applied potentials

Entry	Applied potential, V vs. RHE	Product, $\mu\text{mol}$ (FE, %)			$j$ , $\text{mA cm}^{-2}$
		HCOO <sup>-</sup>	CO	H <sub>2</sub>	
1	-0.47	239 (92)	34 (13)	13 (5.0)	7.7
2	-0.42	195 (96)	14 (6.9)	4.6 (2.3)	6.0
3	-0.37	171 (98)	8.2 (4.7)	2.2 (1.2)	5.8
4	-0.32	132 (92)	14 (10)	4.0 (2.8)	4.3
5	-0.27	72 (98)	5.5 (7.9)	1.5 (2.2)	2.2
6	-0.22	33 (95)	3.3 (9.5)	0.9 (2.7)	1.0

Pre-electrolysis at -0.07 V vs. RHE for 10 min; electrolysis for 1 h in a 0.5 M KHCO<sub>3</sub> solution (Drop-casting counts: 2 times for each)

**Table S3** Control experiments for the electrocatalytic CO<sub>2</sub> reduction operated at -0.27 V vs. RHE for 3 h in a CO<sub>2</sub>-saturated 0.5 M KHCO<sub>3</sub> solution using a [Mes-IrPPh<sub>2</sub>] electrode

Entry	Conditions	Product, $\mu\text{mol}$ (FE, %)			$j$ , $\text{mA cm}^{-2}$
		HCOO <sup>-</sup>	CO	H <sub>2</sub>	
1	Standard	198 (86)	14 (6.1)	6.0 (2.6)	2.3
2	without Ir catalyst	0 (0)	0 (0)	0.4 (0.8)	$7.5 \times 10^{-4}$
3	without carbon black	1.7 (15)	1.2 (11)	0.5 (4.1)	$2.0 \times 10^{-4}$
4	without pyrrole	0 (0)	0 (0)	0.2 (4.5)	$7.1 \times 10^{-4}$
5	without nafion	79 (93)	4.4 (5.2)	1.3 (1.5)	1.5

Pre-electrolysis at -0.07 V vs. RHE for 10 min (Drop-casting counts: 2 times for each)

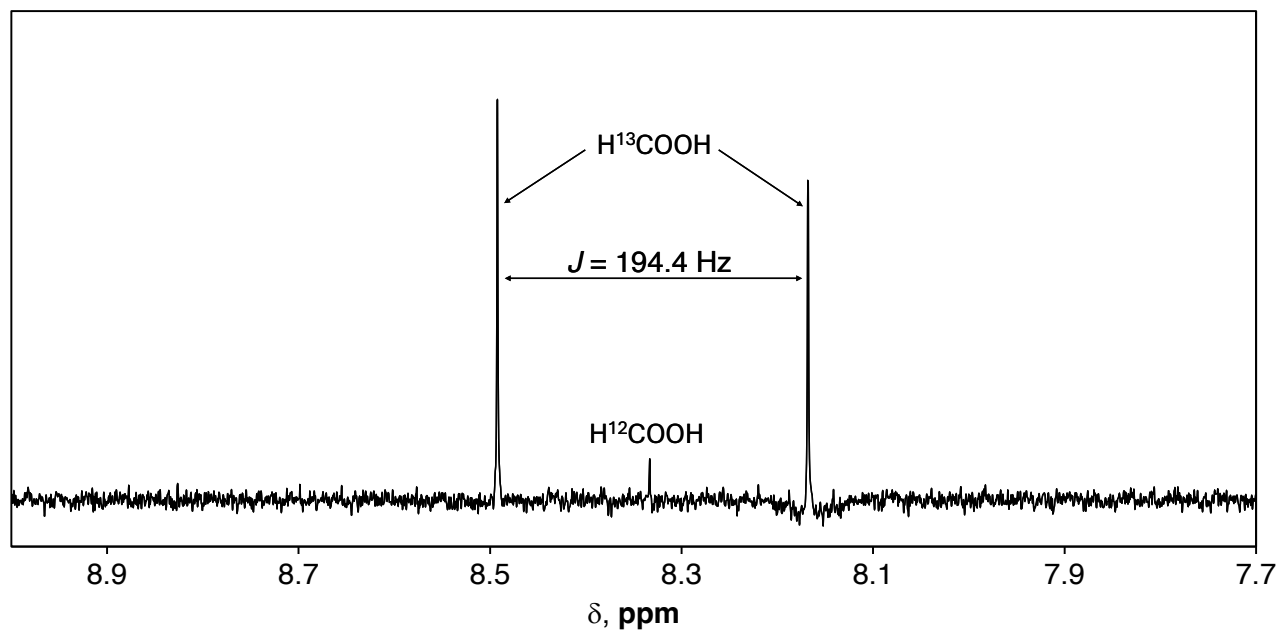


**Fig. S6**  $^1H$  NMR spectra of the reaction solution for  $^{13}CO_2$  labeling experiments obtained during the electrocatalytic  $CO_2$  reduction at  $-0.37$  V vs. RHE for 24 h using a [Mes-IrPPh<sub>2</sub>] electrode in a solution of  $CO_2$ -saturated 0.25 M  $K_2^{13}CO_3$  in  $D_2O$ .

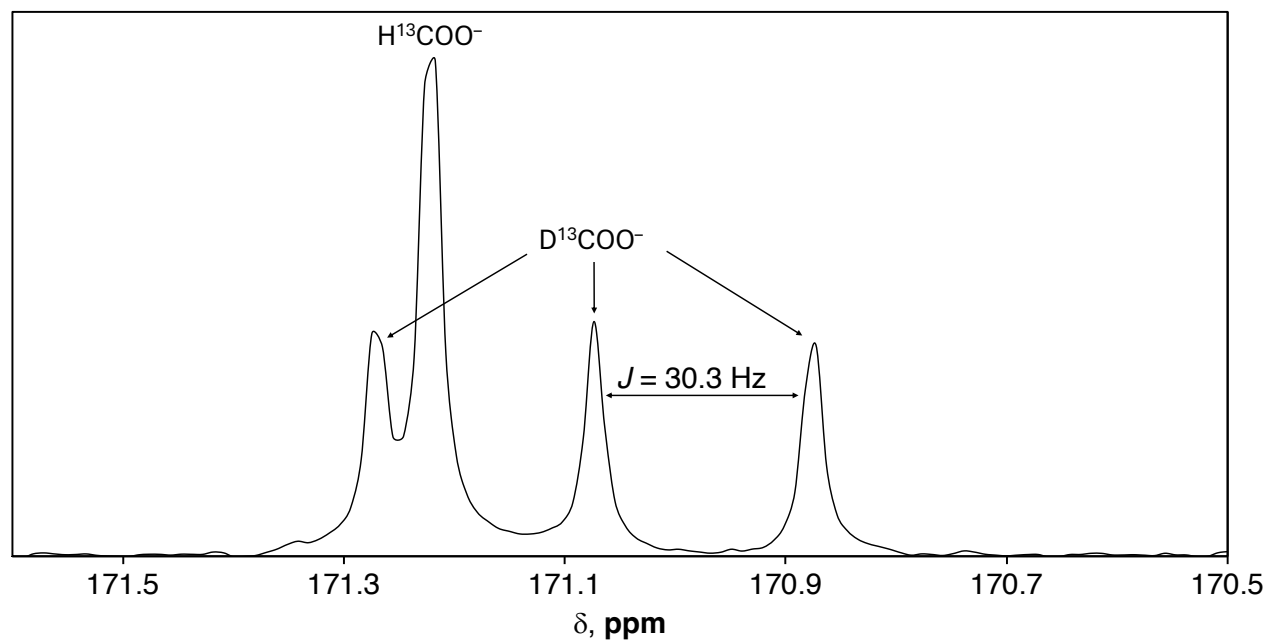


**Fig. S7**  $^{13}\text{C}$  NMR spectra of the reaction solution for  $^{13}\text{CO}_2$  labeling experiments obtained during the electrocatalytic  $\text{CO}_2$  reduction at  $-0.37 \text{ V vs. RHE}$  for 24 h using a **[Mes-IrPPh<sub>2</sub>]** electrode in a solution of  $^{13}\text{CO}_2$ -saturated 0.25 M  $\text{K}_2^{13}\text{CO}_3$  in  $\text{D}_2\text{O}$ .

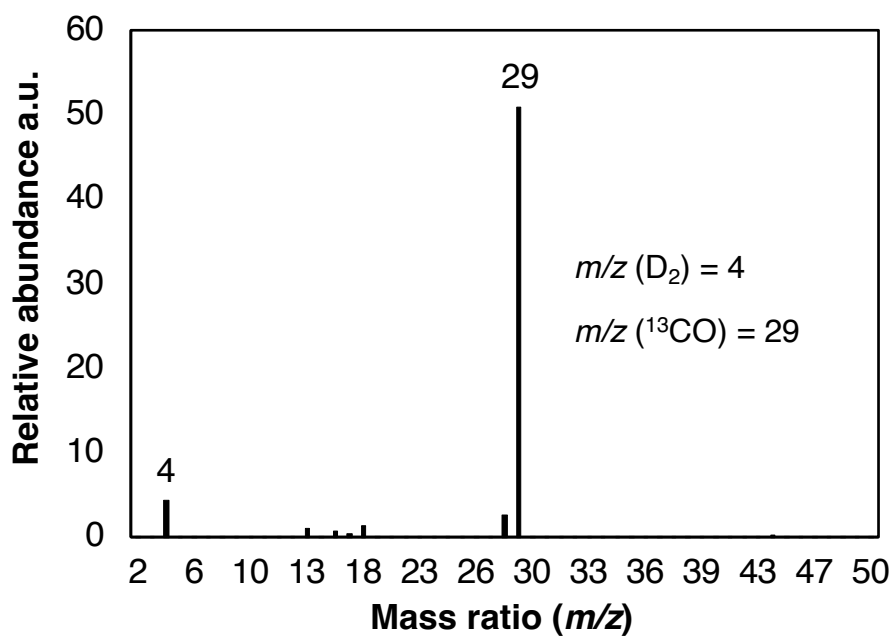
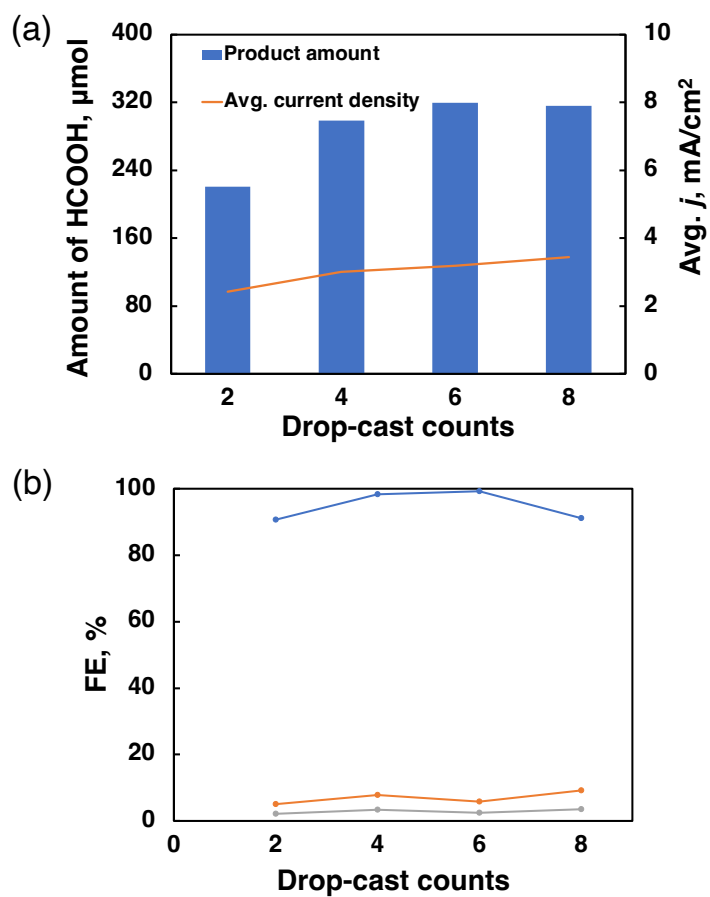


**Fig. S8** Mass spectra of gaseous products for  $^{13}CO_2$  labeling experiments obtained during the electrocatalytic  $CO_2$  reduction at  $-0.37$  V vs. RHE for 24 h using a [Mes-IrPPh<sub>2</sub>] electrode in a solution of  $^{13}CO_2$ -saturated 0.25 M  $K_2^{13}CO_3$ .

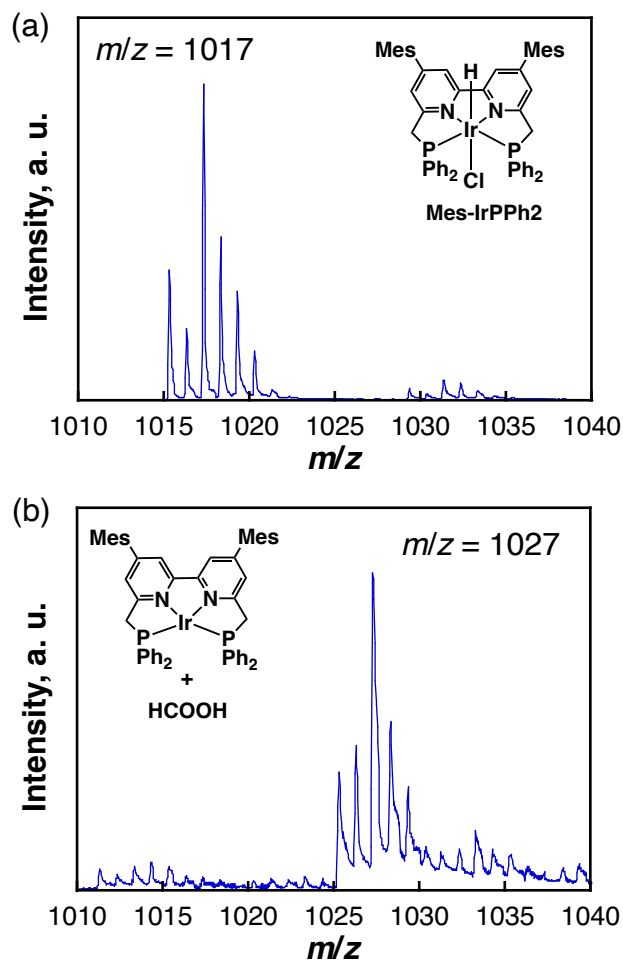
**Table S4** Electrocatalytic CO<sub>2</sub> reduction with a [Mes-IrPPPh<sub>2</sub>] electrode with different drop-cast counts operated at -0.27 V vs. RHE for 3 h in a CO<sub>2</sub>-saturated 0.5 M KHCO<sub>3</sub> solution

Entry	Drop-cast counts	Product, $\mu\text{mol}$ (FE, %)			$j$ , $\text{mA cm}^{-2}$
		HCOO <sup>-</sup>	CO	H <sub>2</sub>	
1	2 times	221 (91)	12 (5.1)	5.5 (2.2)	2.4
2	4 times	298 (98)	24 (7.8)	10 (3.4)	3.0
3	6 times	319 (99)	19 (5.8)	7.9 (2.5)	3.2
4	8 times	316 (91)	32 (9.2)	12 (3.5)	3.4

Pre-electrolysis at -0.07 V vs. RHE for 10 min



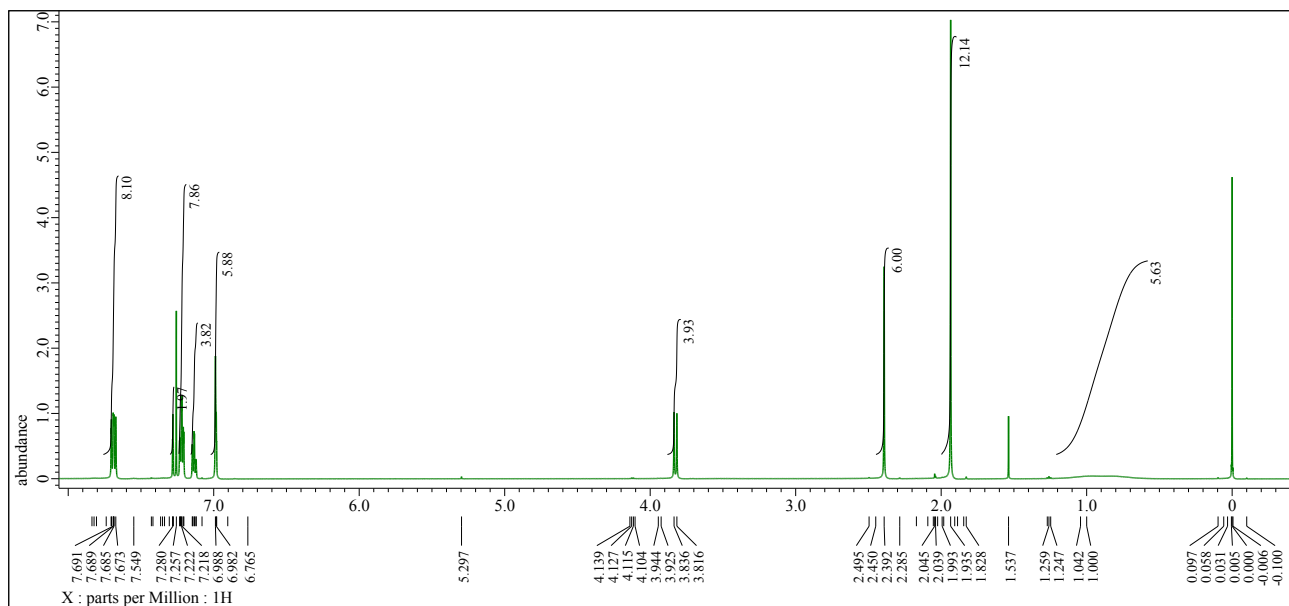
**Fig. S9** Effects of the drop-cast counts on (a) the amount of HCOO<sup>-</sup> and average current densities, and (b) Faradaic efficiency [HCOO<sup>-</sup> (blue), CO (orange), H<sub>2</sub> (gray)].



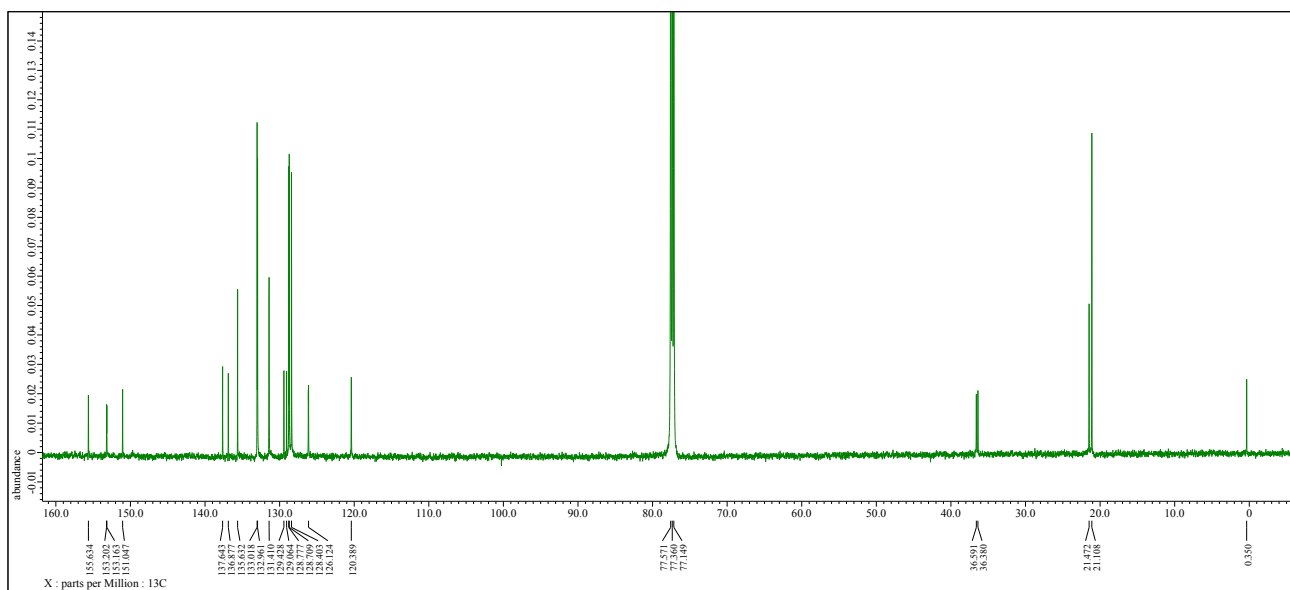
**Fig. S10** ESI-MS spectra of a [Mes-IrPPh<sub>2</sub>] electrode (a) before and (b) after electrocatalytic CO<sub>2</sub> reduction for 72 h at -0.27 V vs. RHE in a solution of CO<sub>2</sub>-saturated 0.5 M KHCO<sub>3</sub>.

**Table S5** Comparison of configurations and performance characteristics for solar CO<sub>2</sub> electrolysis to produce HCOOH by photovoltaic (PV) cell + electrochemical systems

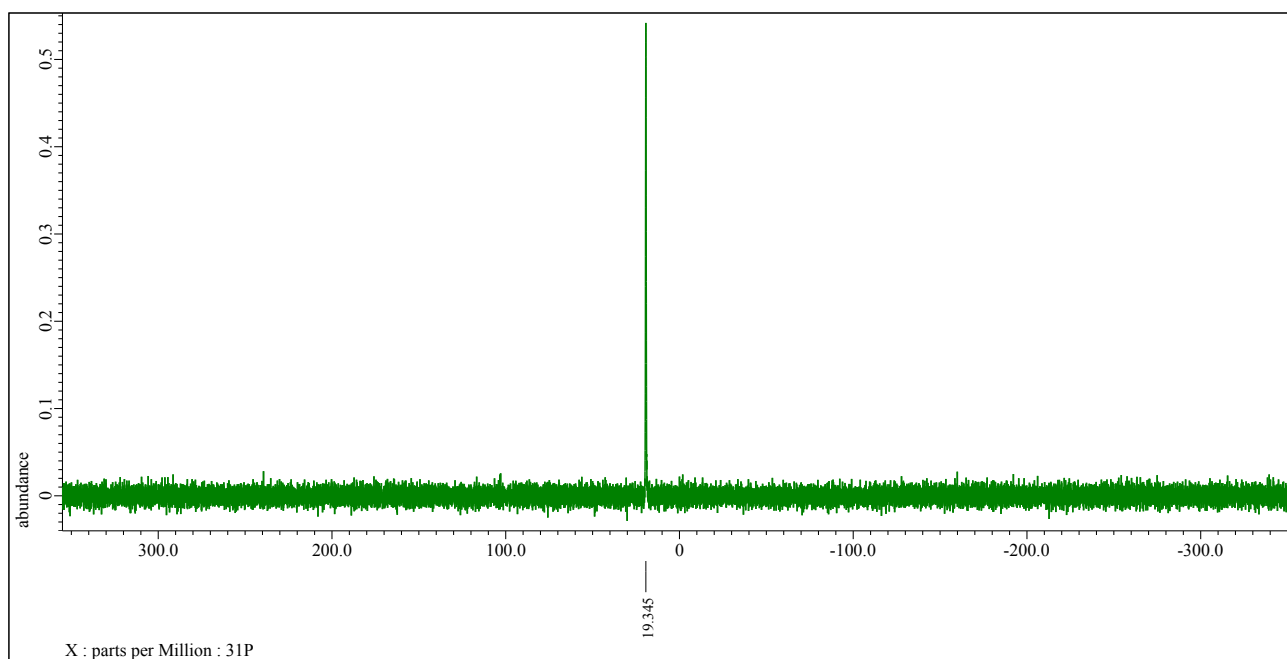
Ref.	$\eta_{\text{STF}}$ , %	PV cell	$\eta_{\text{PV}}$ , %	Cathode Catalysts	Anode Catalysts	Time, h	Full-cell potential, V	Electrolyte
<b>This work</b>	<b>13.7</b>	<b>4Si</b>	<b>22.7</b>	<b>[Mes-IrPPh<sub>2</sub>]</b>	<b>Ni/Fe-Ni foam</b>	<b>24 h</b>	<b>2.10</b>	<b>0.5 M KHCO<sub>3</sub></b>
S4	7.20	c-Si	–	Ti/graphite/CS/MWCNTs/RuCP	FTO/Ag/IrO <sub>x</sub>	3 h	1.85	0.4 M KPi
S5	10.5	c-Si	–	Ti/graphite/CS/MWCNTs/RuCP	Ti/IrO <sub>x</sub>	3 h	1.65–1.69	0.4 M KPi
S6	14.3	GaInP/GaAs/Ge	29.0	g-In <sub>2</sub> S <sub>3</sub>	Ni/Fe-LDH	3 h	2.20	2.0 M KHCO <sub>3</sub>
S7	13.7	GaInP/GaAs/Ge	–	Cu-Bi	NiFe	8 h	2.02	0.5 M KHCO <sub>3</sub>
S8	13.3	GaInP/GaAs/Ge	28.5	BiNN-CFs	RuO <sub>2</sub>	4 h	2.55	1.0 M KOH
S9	11.8	GaInP/GaAs/Ge	25.2	B-Bi	FeP	4 h	2.46	0.5 M KHCO <sub>3</sub>
S10	13.3	GaInP/GaAs/Ge	23.0	BOC with V <sub>o</sub>	MoNi <sub>0.05</sub> F <sub>e<sub>0.05</sub></sub> O <sub>2</sub>	8 h	2.10	0.5 M KHCO <sub>3</sub>



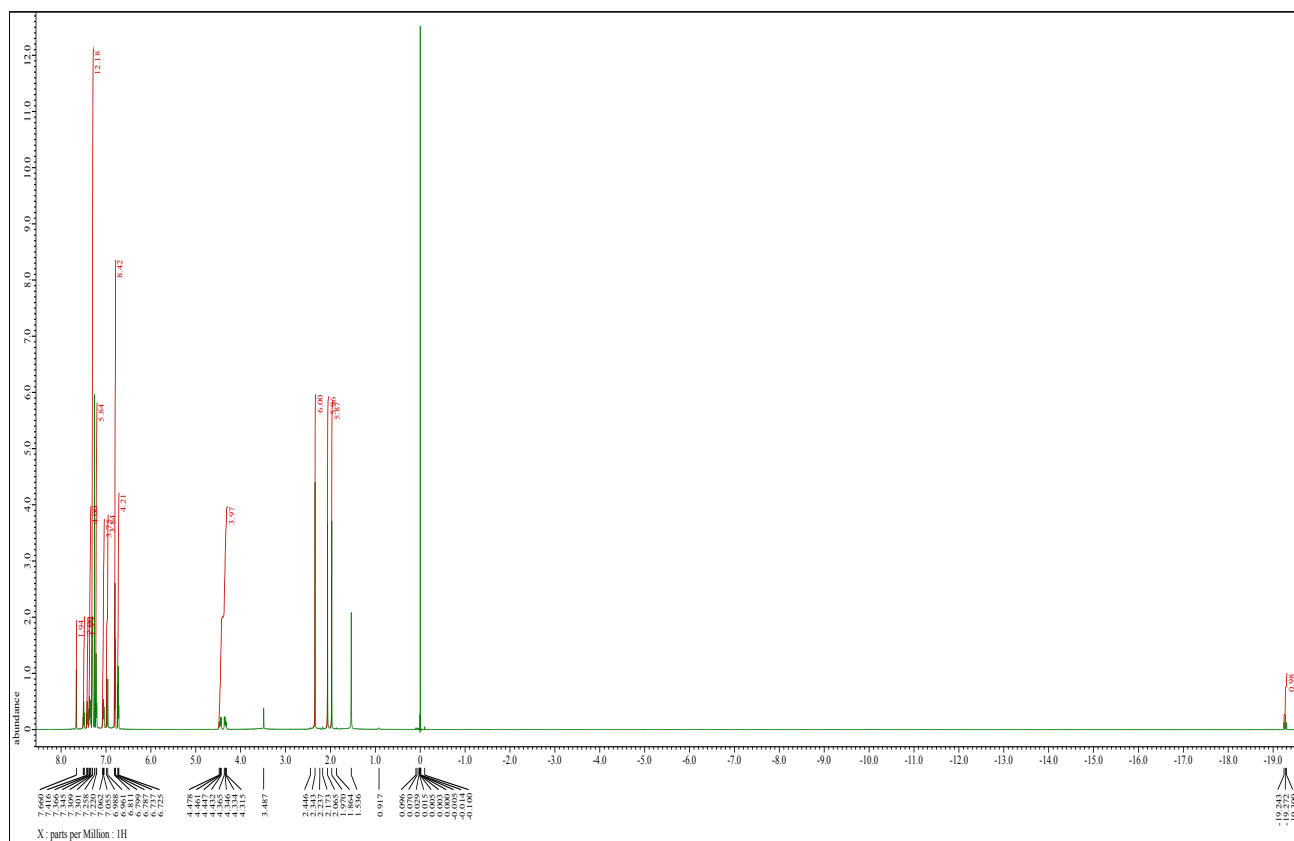
**Fig. S11**  $^1\text{H}$  NMR spectrum (solvent:  $\text{CDCl}_3$ ) of **3**.



**Fig. S12**  $^{13}\text{C}\{^1\text{H}\}$  NMR spectrum (solvent:  $\text{CDCl}_3$ ) of **3**.



**Fig. S13**  $^{31}\text{P}\{^1\text{H}\}$  NMR spectrum (solvent:  $\text{CDCl}_3$ ) of **3**.



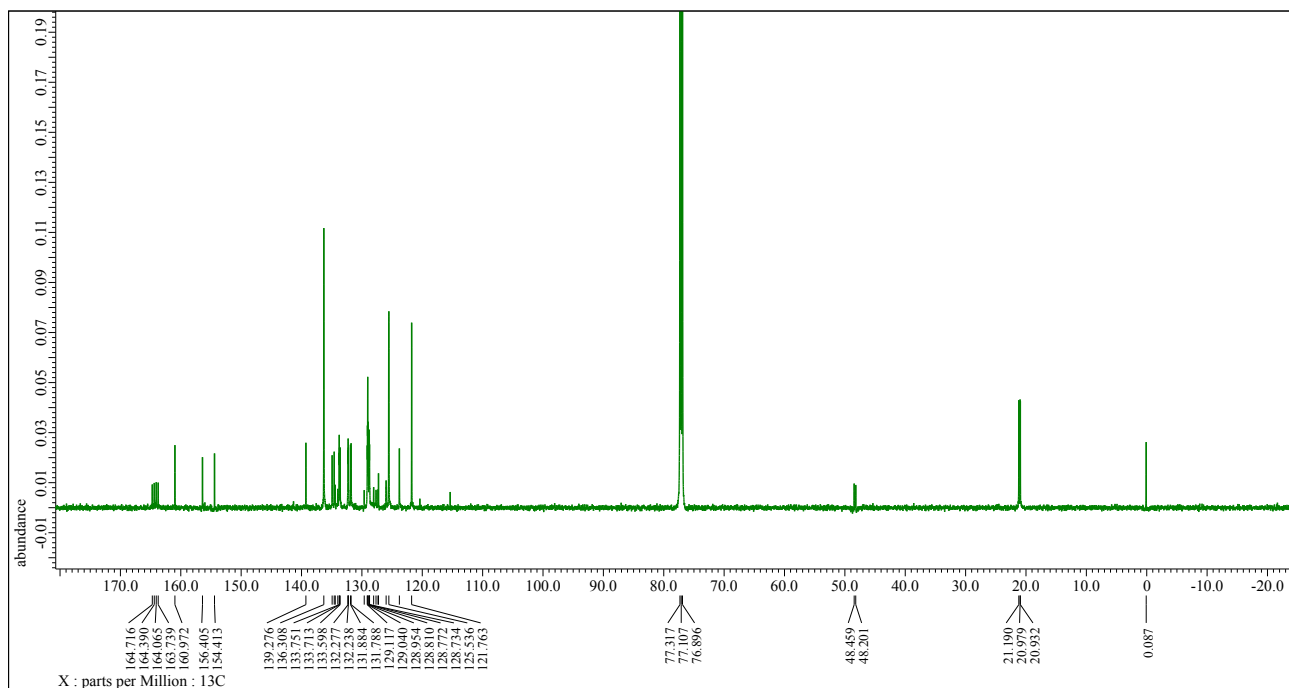


**Fig. S15**  $^{13}\text{C}\{^1\text{H}\}$  NMR spectrum (solvent:  $\text{CDCl}_3$ ) of **Mes-IrPPh<sub>2</sub>**.

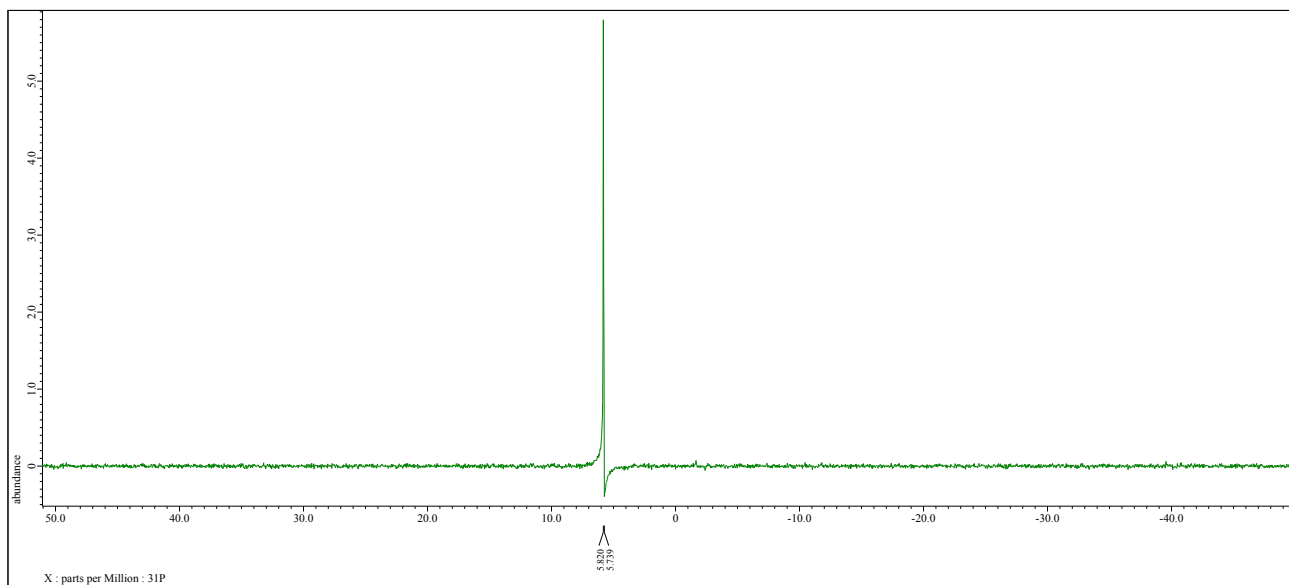


**Fig. S16**  $^{31}\text{P}\{^1\text{H}\}$  NMR spectrum (solvent:  $\text{CDCl}_3$ ) of **Mes-IrPPh<sub>2</sub>**.

## References

- S1 S. Yoshioka, S. Nimura, M. Naruto and S. Saito, *Sci. Adv.*, 2020, **6**, eabc0274.
- S2 K. Kamada, J. Jung, T. Wakabayashi, K. Sekizawa, S. Sato, T. Morikawa, S. Fukuzumi and S. Saito, *J. Am. Chem. Soc.*, 2020, **142**, 10261–10266.
- S3 S. Sato, K. Sekizawa, S. Shirai, N. Sakamoto and T. Morikawa, *Sci. Adv.*, 2023, **9**, eadh9986.
- S4 N. Kato, S. Mizuno, M. Shiozawa, N. Nojiri, Y. Kawai, K. Fukumoto, T. Morikawa, Y. Takeda, *Joule*, 2021, **5**, 687–705.
- S5 N. Kato, Y. Takeda, Y. Kawai, N. Nojiri, M. Shiozawa, S. Mizuno, K. Yamanaka, T. Morikawa and T. Hamaguchi, *ACS Sustainable Chem. Eng.*, 2021, **9**, 16031–16037.
- S6 Q. Zhang, J. Gao, X. Wang, J. Zeng, J. Li, Z. Wang, H. He, J. Luo, Y. Zhao, L. Zhang, M. Grätzel and X. Zhang, *Joule*, 2024, **8**, 1–19.
- S7 Z. Li, B. Sun, D. Xiao, Z. Wang, Y. Liu, Z. Zheng, P. Wang, Y. Dai, H. Cheng and B. Huang, *Angew. Chem. Int. Ed.*, 2023, **62**, e202217569.
- S8 B. Wulan, L. Zhao, D. Tan, X. Cao, J. Ma, J. Zhang, *Adv. Energy Mater.* 2022, **12**, 2103960.
- S9 X. Chen, H. Chen, W. Zhou, Q. Zhang, Z. Yang, Z. Li, F. Yang, D. Wang, J. Ye and L. Liu, *Small*, 2021, **17**, 2101128.
- S10 X. Chen, J. Chen, H. Chen, Q. Zhang, J. Li, J. Cui, Y. Sun, D. Wang, J. Ye and L. Liu, *Nat. Commun.*, 2023, **14**, 751.